

# Toward Industrially Feasible Methods for Following the Process of Manufacturing Cellulose Nanofibers

Carl Moser,<sup>a,b,\*</sup> Mikael E. Lindström,<sup>a</sup> and Gunnar Henriksson<sup>a</sup>

Nanocellulose is a recently developed form of cellulose that has the potential to be used in many different industries, ranging from food to high-performance applications. This material is commercially manufactured through the homogenization of chemical pulps, but the process is energy-consuming and is still an important subject for development. Simple, robust methods are required for the quality control and optimization of industrial nanocellulose production. In this study, a number of different methods, based on different principles of monitoring the manufacture of cellulose nanofibers were evaluated and compared for five different nanocellulose qualities, both for their resolution and robustness/ease. Methods based on microscopy, light scattering, centrifugation, and viscosity were examined and all appeared useful for observing the manufacturing process during its initial stage. However, only methods based on centrifugation, turbidity, and transmittance yielded reliable data for the entire manufacturing process. Of these methods, transmittance measurement may be the best candidate for routine use because the method is simple, rapid, and only requires spectrophotometer equipment.

*Keywords:* Cellulose nanofibers; Microfibrillated cellulose; Nanofibrillated cellulose; Characterization; Transmittance; Turbidity

*Contact information:* a: Department of Fibre and Polymer Technology, School of Chemistry, Royal Institute of Technology, KTH, Teknikringen 56-58, 10044 Stockholm, Sweden; b: Valmet AB, 851 94 Sundsvall, Sweden; \*Corresponding author: cmoser@kth.se

## INTRODUCTION

Throughout the past few decades, there have been two main trends in materials development. The first is the development of materials based on renewable resources, which is of importance not only in reaching a sustainable technical culture independent of non-renewable resources such as petroleum, but also for environmental reasons. Non-biodegradable materials (*i.e.*, petroleum-based particles) are being accumulated in nature and have potentially negative effects on living organisms. The second trend is the use of nanotechnology, including nanofibers, to produce materials with novel, interesting properties. It is not surprising that the combination of these two trends in the field of nanoparticles made from wood has caused an exponential increase in the number of related publications (Siró and Plackett 2010; Ankerfors 2012) since microfibrillated cellulose (MFC) was first discovered in the late 1970s (Herrick *et al.* 1983; Turbak *et al.* 1983; Herrick 1984).

Cellulose, the most common biopolymer on Earth (Klemm *et al.* 2005; Wilson *et al.* 2012; Brinchi *et al.* 2013), is composed of  $\beta$ -(1 $\rightarrow$ 4)-D-glucopyranose units (Meshitsuka and Isogai 1995) linearly arranged into elementary fibrils with lateral dimensions of 3 to 5 nm (Meier 1962; Ohad and Danon 1964; Heyn 1969; Blackwell and

Kolpak 1975) and lengths of a few microns (Klemm *et al.* 2005, 2011; Siró and Plackett 2010). These fibrils have segments with lower crystallinity and higher reactivity (Blackwell and Kolpak 1975; Henriksson *et al.* 2007b; Pääkkö *et al.* 2007). Agglomeration into microfibrillar aggregates reduces the surface energy of the elementary fibrils (Peterlin and Ingram 1970), and the subsequent bundles have lateral dimensions of 10 to 35 nm (Frey-Wyssling *et al.* 1948; Meier 1962; Heyn 1969). These aggregates are organized in higher hierarchical levels that eventually, in combination with lignin and hemicelluloses, form cell walls and are known as “fibers”, as shown in Fig. 1 (Mühlenthaler 1949).

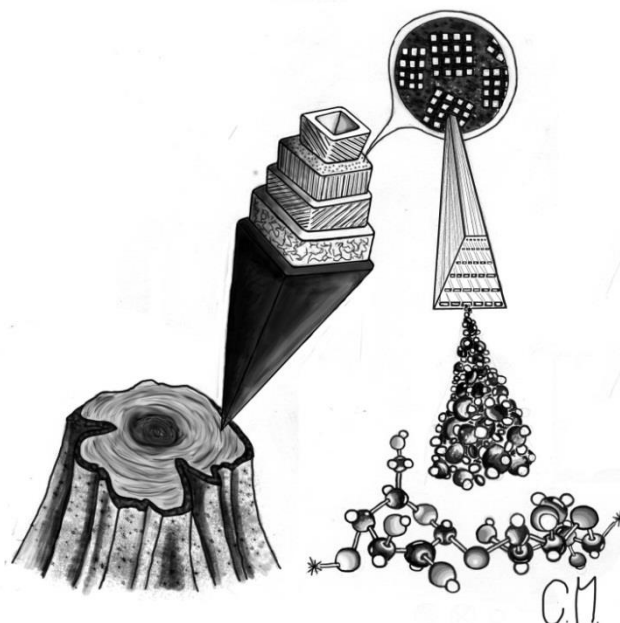


**Fig. 1.** Representation of the fiber hierarchy in softwood from a single fiber, showing the middle lamellae, primary layer, S1, S2, S3, and lumen. A magnification shows fibrillar bundles in the S2 layer surrounded by lignin and hemicelluloses. An elementary fibril, including its 36 linearly-arranged cellulose chains, is also shown, with an illustration of the repeating unit cellobiose.

Cellulose in lower hierarchical levels, such as fibrillar aggregates or individual fibrils, can be released from the cell wall and form nanofibrils or nanoparticles that can be utilized in different applications. This can be achieved in several ways: elementary cellulose nanocrystals (CNC) can be isolated by removing the semicrystalline cellulosic regions in a low-yield (21 to 38%; (Hamad and Hu 2010)) process in which a bleached, refined pulp is hydrolyzed in mineral acids (Nickerson and Harble 1947; Rånby 1949; Rånby 1951). The released cellulose nanocrystals have lateral dimensions of approximately 7 nm and lengths on the order of 100 to 300 nm depending on the duration of hydrolysis and degree of polymerization (DP) of the original cellulose source ( Dong *et al.* 1996; Beck-Candanedo *et al.* 2005; Elazzouzi-Hafraoui *et al.* 2008).

Elementary fibrils and microfibrillar aggregates can be derived by subjecting a pulp of low consistency to mechanical disintegration, commonly performed in either a homogenizer (Herrick *et al.* 1983; Turbak *et al.* 1983) or microfluidizer (Pääkkö *et al.* 2007). The product possesses a high aspect ratio with widths of approximately 5 to 60 nm (Herrick *et al.* 1983; Turbak *et al.* 1983; Herrick 1984; Fall *et al.* 2011) and lengths of a few micrometers, making them flexible compared to CNC (Siró and Plackett 2010;

Klemm *et al.* 2011). Ambiguous terms can sometimes cause confusion. The term first coined was microfibrillated cellulose (MFC) (Herrick *et al.* 1983; Herrick *et al.* 1983; Turbak *et al.* 1983; Herrick 1984), which refers to a material with large inhomogeneity, whereas newer terms, such as nanofibrillated cellulose (NFC) (Iwamoto *et al.* 2008) and cellulose nano filaments, fibrils, or fibers (CNF) (Langlois *et al.* 2002; Jin *et al.* 2004; Hua *et al.* 2011), refer to a material with smaller lateral dimensions.

Mechanical comminution of untreated fibers into a nanomaterial requires 70 to 100 MWh/t, a considerable amount of energy (Turbak *et al.* 1983; Eriksen *et al.* 2008; Saito *et al.* 2009; Siró and Plackett 2010). Two main pathways have been explored to lower the energy input including fiber pretreatments (Henriksson *et al.* 2007b; Saito *et al.* 2007; Tejado *et al.* 2012) and the implementation of novel disintegration techniques (Chatterjee and Makoui 1984; Wang and Sain 2007; Alemdar and Sain 2008). Pretreatments typically swell the fibers, facilitating disintegration and increasing the yield of nanoparticles. A monocomponent endoglucanase enzyme is capable of the specific hydrolysis of the glucosidic bonds along the cellulose chain, located particularly in the less crystalline areas (Henriksson *et al.* 2005). From a structural perspective, cellulose nanofibers produced from enzymatically-treated fibers have lateral dimensions in two distinct ranges: 5 to 8 nm and 12 to 25 nm (Henriksson *et al.* 2007a; Pääkkö *et al.* 2007). Increasing the anionic charge density induces electrostatic repulsion, which causes swelling (Isogai *et al.* 2011); the charge density is directly proportional to the mechanical energy input, with a higher charge density decreasing the energy required (Tejado *et al.* 2012). One approach to increasing charge density is catalytic oxidation with 2,2,6,6-tetramethylpiperidine-1-oxyl radicals (TEMPO) (Saito *et al.* 2006, 2007). A threshold can be observed at 0.6 mmol/g carboxyl groups, above which the predominant lateral dimension is 3 to 5 nm with lengths of 2  $\mu\text{m}$  or more after homogenization (Saito *et al.* 2009; Isogai *et al.* 2011). However, there is still need for improvement in the manufacturing process for cellulose nanofibers, both in obtaining cost-efficient production and in producing cellulose nanofibers with specific qualities. The problem with such process development is the lack of simple characterization methods for monitoring the cellulose nanofiber manufacturing process (Chinga-Carrasco *et al.* 2013). Furthermore, robust and relatively simple methods for CNC characterization are needed for product quality control during the industrial production of nanocellulose.

There is a need to quantify the process of disintegrating pulp fibers into cellulose nanofibers. Because the goal is to fragment pulp fibers into nanofibers, it is preferable to detect the formation of nanofibers (*i.e.*, smaller particles). Direct detection requires some form of microscopy. This is problematic because the nanofibers are too small to be visible with normal light microscopy and instead require electron or atomic force microscopy (AFM). Microscopy has indeed been widely utilized to determine the lateral dimensions and lengths of cellulose nanofibers. The most common methods are field-emission scanning electron microscopy (FE-SEM) (Zimmermann *et al.* 2004; Chakraborty *et al.* 2005; Abe *et al.* 2007; Iwamoto *et al.* 2007; Wang and Sain 2007; Alemdar and Sain 2008; Kaushika and Singh 2011; Qua *et al.* 2011), transmission electron microscopy (TEM) (Alemdar and Sain 2008; Chakraborty *et al.* 2005; Kaushika and Singh 2011; Pääkkö *et al.* 2007; Qua *et al.* 2011; Saito *et al.* 2009; Wang and Sain 2007; Zimmermann *et al.* 2004), and atomic force microscopy (AFM) (Chakraborty *et al.* 2005; Pääkkö *et al.* 2007; Wang and Sain 2007; Kaushika and Singh 2011; Helander *et al.* 2012). Although veracious size measurements can be performed at the nano-scale, only a limited field of view is visualized, often overlooking larger structures (Chinga-

Carrasco 2013). However, the quantification of microscopic data is tedious, and it may be difficult to obtain data representative of the small samples analyzed. The use of imaging tools such as UTHSCSA (Kaushika and Singh 2011) facilitates more quantitative measurements. Nevertheless, fractional yields cannot be obtained. One possibility is the use of automatic microscopy combined with image analysis software such as those associated with Kajaani and Fibermaster devices. However, cellulose nanofibers are below the detection limit of the standard versions of these methods.

It is also possible to use indirect methods to monitor the disintegration process. One such method is measuring the larger particle content, which can be done in several ways. Measuring equipment such as microscopy/Fibermaster/KajaaniFiberLab can be used to investigate the elimination of larger particles at a given mass concentration. Using a similar principle, one could also monitor what fraction of a material can penetrate a filter. Dead-end filtration has issues with filter cake formation, so agitated filtration, such as with a Britt Dynamic Drainage Jar, could be a better alternative.

The change in various physical properties of the pulp/nanofiber suspension can also be monitored by methods such as centrifugation that rely on the fact that larger particles of similar density sediment faster in a given gravitational field than smaller particles. Smaller particles remain in the supernatant, whereas larger particles end up in the pellet. Thus, a decrease in the amount of a suspension that can be pelleted under given centrifugation conditions can be used to monitor the manufacturing process of cellulose nanofibers. The gravimetric yield of nanofibers was shown to be directly dependent on the charge density of the sample, with a higher charge causing less precipitation due to increased colloidal stability (Fall *et al.* 2011). The use of a rotational fractioning device containing interchangeable screens, with pore sizes ranging from 20 to 0.1  $\mu\text{m}$ , was determined to be capable of separating the material into size fractions (Tanaka *et al.* 2012b). However, the morphologies of these fractions were not determined.

Particles below a certain size do not scatter light. This is true for cellulose nanofibers, so a decrease in light scattering and an increase in the transmittance (*i.e.*, the transparency of a solution or film) can also be used to monitor the manufacturing process of cellulose nanofibers. Spectroscopic methods have been employed to evaluate the degree of fibrillation by measuring the transmittance or turbidity of the solution. Transmittance has been measured on films using UV-visible spectrometry (Iwamoto *et al.* 2008; Fukuzumi *et al.* 2009; Aulin *et al.* 2010) or dynamically by flow (Chinga-Carrasco 2013). Turbidity is a vital parameter used to evaluate waste water quality in the pulp and paper industry (Pokhrel and Viraraghavan 2004). It measures the amount of particles in a liquid by analyzing the extent of light scattered. It is possible to correlate turbidity (inversely) and transmittance (directly) to the degree of fibrillation. Light scattering can be neglected for liquids containing nanoparticles below their agglomeration concentration (Jukka *et al.* 2004).

Dynamic light scattering (DLS) measures the spherical volume enclosing a nonmoving nanoparticle (*i.e.*, the hydrodynamic radius) (Fall *et al.* 2011). A hydrodynamic radius distribution can be considered the particle size distribution (Tanaka *et al.* 2012a) for spherical particles. DLS has limitations when larger particles are considered because the measurements cannot be performed accurately (Tanaka *et al.* 2012a). The hydrodynamic radius of cellulose nanofibers is expected to change with lateral size, length, and charge density.

A liquid's resistance to shear or flow can be used to evaluate the degree of fibrillation because the viscosity, storage, and loss modulus decrease with the number of

homogenization passes (Winuprasith and Suphantharika 2013), while an increase in charge density increases the viscosity (Zhang *et al.* 2012). Cellulose nanofibers exhibit non-Newtonian, pseudoplastic liquid characteristics with shear-thinning properties (Gousse *et al.* 2004; Moberg and Rigdahl 2012; Zhang *et al.* 2012) that consequently depend on the shear rate and concentration (Moberg and Rigdahl 2012; Rezayati Charani *et al.* 2013).

The objective of this work was to examine and compare a number of methods, based on atomic force microscopy, filtration, centrifugation, transmittance, turbidity, dynamic light scattering, and viscosity, for characterizing nanocellulose. The goal was to collect information sufficient to determine which methods to use to evaluate different nanocellulose manufacturing processes.

In this work, nanocellulose manufactured by homogenization with different degrees of intensity, following either endoglucanase or TEMPO oxidation pretreatments, was used. A sample of nanocellulose manufactured using another technique, nanopulping (Helander *et al.* 2012), was also included.

## EXPERIMENTAL

### Materials

The raw material for the production of cellulose nanofiber was a commercial, never-dried softwood pulp (SCA Östrand, SE) with hemicellulose content 16.7% and lignin content 0.65%.

#### *Preparation of nanofibers*

The chemical reactivity was increased with high consistency refining at 230 kWh/t. Disintegration was facilitated either by enzymatic hydrolysis with an endoglucanase enzyme (FiberCare®, Novozymes, DE) at 24.8 ECU/g and 55 °C for 1 h (Henriksson *et al.* 2005, 2007a; Pääkkö *et al.* 2007) or by increasing the charge density from 50 to 443 µmol/g (measured by conductimetric titration) (Katz *et al.* 1984) using a TEMPO (15.6 mg/g, 2,2,6,6-tetramethyl-piperidinyloxy, Sigma-Aldrich Sweden AB, SE) mediated oxidation with sodium chlorite (1.13 g/g, Sigma-Aldrich Sweden AB, SE) and sodium hypochlorite (1 mL/g at 10%, Sigma-Aldrich Sweden AB, SE) at 60 °C for 16 h (Saito *et al.* 2009).

The pretreated fibers were mechanically disintegrated in a Microfluidizer (M-110EH, Microfluidics Corp, US) at 10 g/L using two large chambers in series (400 and 200 µm, respectively) at 925 bar for the first pass and smaller chambers (200 and 100 µm, respectively) at 1600 bar for one or five passes for each pretreatment, generating four different products: enzyme one pass, enzyme five passes, TEMPO one pass, and TEMPO five passes. The corresponding energy consumption of one and five passes were approximately 7000 and 25000 kWh/t, respectively, as calculated according to methods described in a previous report (Ankerfors 2012).

A fifth quality was obtained *via* nanopulping, a steam explosion concept, with approximate energy consumption of 700 kWh/t without steam heat recovery (Helander *et al.* 2012). The energy consumption during pretreatments was not taken into account for either sample. Macroscopic effects were visualized using light optical microscopy, as shown in

Fig. 2.

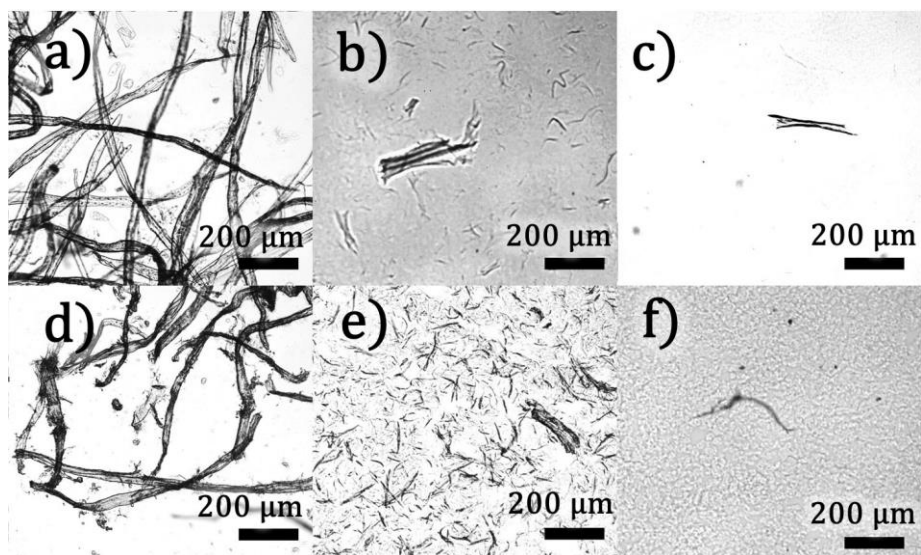


**Fig. 2.** Light optical microscopic images of a) untreated reference, b) TEMPO one pass, c) TEMPO five passes, d) nanopulp, e) enzyme one pass, and f) enzyme five passes

## Methods

### Centrifugation

Centrifugation was performed on all samples (pH  $7 \pm 0.1$ ) with a concentration of 1.5 g/L at 9800 RCF (relative centrifugal force) for 45 min in either a table centrifuge (Minispin Plus, Eppendorf AB, GE) using 2-mL samples or a larger centrifuge (Beckman coulter®, US) using 30-mL samples. The gravimetric yield was calculated as the amount of stable nanofibers in the supernatant after centrifugation by (Eq. 1),

$$\text{Yield} = 1 - m_p / m_{tot} \quad (1)$$

where  $m_p$  is the weight of the pellet and  $m_{tot}$  is the total weight of the sample (Wågberg *et al.* 2008). The samples were dispersed in deionized water from 10 to 1.5 g/L using different methods prior to centrifugation to investigate the effects on gravimetric yield; 200-mL samples were dispersed using magnetic stirring for 20 h at maximum intensity, Ultra-Turrax (®T25 digital, IKA, GE) for 1 to 120 min at 8000 rpm, homogenization (Microfluidizer M-110EH, Microfluidics Corp, US) using a series of chambers 400 and 200  $\mu\text{m}$  in size at a pressure of 1000 bar, or by probe ultrasonication (Vibra-Cell, Sonics, US) for 10 min at 70% intensity.

### Macro-fraction and FiberLab

A macro-fraction was determined using a modified Britt Dynamic Drainage Jar (BDDJ) (PRM Inc., US) procedure. A 200-mL sample containing 1 g/L fiber was added to a BDDJ. The mixer was set to 422 rpm, and the valve, 5 mm, was opened. The sample was continuously diluted with deionized water to maintain a total of 1 L. The fibers remaining on the metal filter (0.125 p) were weighed as the macro-fraction. Size averages of the macrofraction were determined using FiberLab (Metso, FI).

### Dynamic light scattering (DLS)

DLS (Zetasizer ZEN3600, Malvern Instruments, UK) was employed to determine the hydrodynamic radii of the nanofibers in the supernatants from the different qualities.

Measurements were performed on 1-mL samples at 0.1 g/L to remain below an overlap concentration.

#### *Atomic force microscopy (AFM)*

Glow-discharged silica wafers with an anchoring layer of PEI (polyethyleneimine), with molecular weight 25 kDa and pH 8, were used to adsorb the nanofibers from centrifugal supernatants at approximately 0.2 g/L. The AFM analysis was performed in a Multimode 8 apparatus (Bruker, US) using ScanAsyst.

#### *Transmittance*

The absorbance was measured in an UV-vis spectrophotometer (UV-2550, Shimadzu, JP) in the wavelength range of 200 to 800 nm ( $A_{200-800}$ ) and converted to transmittance by Eq. 2:

$$T_i = 100 \times 10^{-A_i} \quad (2)$$

Measurements were performed on samples in deionized water at a concentration of 1.5 g/L. The concentration dependence was evaluated for enzyme one pass within the range 2 to 0.1 g/L.

#### *Turbidity*

The turbidity was measured on a 30-mL sample at 1 g/L in a turbidimeter (2100AN IS Turbidimeter [ISO 7027], HACH, US). Air bubbles were removed by submerging the turbidimeter vials in an ultrasonication bath (ULTRASONIK 28x, CiAB, SE) for 10 s, after which the samples were turned upside down prior to measurement. The concentration dependence was evaluated by continuous dilution until the turbidity was lower than 1 NTU (Nephelometric Turbidity Unit).

#### *Viscosity*

Viscosity was measured at 1 g/L and 1 to 100 rpm with a rheometer (DV-111 programmable rheometer, Brook Field, US).

#### *Degree of polymerization*

DP ( $\bar{P}_v$ ) was calculated using the Mark-Houwink-Sakurada (MHS) equation (Eq. 3), with  $a$ , 0.806 and  $K'$ , 1.26 mL/g (Evans and Wallis 1989), assuming that the intrinsic viscosity is the same for reacted and native cellulose at the same DP (Mishra *et al.* 2011).

$$[\eta] = K' \bar{P}_v^a \quad (3)$$

## RESULTS AND DISCUSSION

The TEMPO treatment and enzymatic hydrolysis decreased the degree of polymerization (DP) from an initial value of 2200 to 1300 and 800 DP, respectively, consistent with the values reported in literature (Henriksson *et al.* 2007a; Lapierre *et al.* 2006; Saito *et al.* 2009). Homogenization further decreased the DP, and the endoglucanase-treated samples were decreased to 500 DP after one pass and 300 DP after

five passes, whereas the TEMPO sample were decreased to 1000 DP after one pass and to 900 DP after five passes. The chemical composition after homogenization was not studied, since only minor changes are to be expected (Spence *et al.* 2010).

Centrifugation is an effective method for measuring the gravimetric yield in which nanoparticles remain in the supernatant phase. The results were independent of measuring volume as long as the same relative centrifugal force was maintained. Decreasing the pH induced agglomeration for samples above their overlap concentration (Fall *et al.* 2013), increasing their water stability and lowering yield. This was shown by lowering the pH to 2 before subjecting the samples to centrifugation, which resulted in yields of approximately 5 wt.% for the enzymatically-treated samples and 0 wt.% for the TEMPO-oxidized samples. Increasing the concentration had a similar effect, exhibiting higher yields due to increased gel stability.

The gravimetric yield of nanofibers after one pass with enzyme pretreatment (enzyme one pass) was 13.6 wt.% and the macro-fraction was 8.3 wt.% (Fig. 3), indicating the presence of a middle-fraction making up 78.1 wt.% of the mixture. After four additional passes (enzyme five passes), the yield increased to 22.2 wt.% and the macro-fraction was no longer distinguishable, equating to 77.8 wt.% middle-fraction. For this quality, no fibers could be measured using FiberLab, indicating that the middle fraction was too small to be measured using optical methods and that the fibers measured with FiberLab were those discerned by the macro-fraction experiment. Increasing the charge density from 50 mmol/kg (native) to 443 mmol/kg (TEMPO-oxidized) resulted in a gravimetric yield of 84.2 wt.% and a macro-fraction of 1.3 wt.% after one pass and a yield of 99.7 wt.% after five passes, which was significantly larger than in the enzymatically-treated samples. Nanopulp had an 8.7 wt.% yield of nanoparticles and a macro-fraction of 59.8 wt.% with an average length of 310  $\mu\text{m}$ , an 83.8% decrease in average length than that of the reference (1910  $\mu\text{m}$ , measured using FiberLab).

Adequate dispersion is paramount for obtaining accurate yield values, particularly for the TEMPO-oxidized samples, which exhibited higher gel stability than the enzymatically-treated samples. Ultra-Turrax dispersion for 10 min stabilized the yield values in all cases, and prolonged exposure (30 min) did not significantly affect the yield. Further homogenization and ultrasonication increased the yield of TEMPO one pass by 11.8 wt.%, but no substantial effect was noted in the other samples.

Considering the energy requirements per ton of nanofibers (Table 1), achieved *via* nanopulping were lowest, closely followed by TEMPO one pass. This result indicates that the fractionation of a lesser-quality of nanofiber-containing material may be of higher value than continued mechanical comminution.

Transmittance was correlated directly with yield and inversely with turbidity, as shown in Fig. 3. When the amount of detectable particles increased, the turbidity increased and the transmittance decreased until a plateau value was reached. After this point, the generation of nanoparticles is favored, decreasing turbidity and increasing transmittance. However, when performing mechanical disintegration, the release of nanoparticles occurs simultaneously with the release of detectable particles, making it difficult to use this method alone to determine the degree of disintegration. Both methods are also sensitive to differences in concentration. Nevertheless, both methods exhibited greater sensitivity than centrifugation. Only TEMPO one pass exhibited any increase in yield after homogenization, whereas all samples showed large changes in turbidity and transmittance. Turbidity decreased by 41% for enzyme one pass, 50% for enzyme five passes, 90% for TEMPO one pass, and 73% for TEMPO five passes, while increasing by



60% for nanopulp after homogenization. The increase in the nanopulp turbidity was because that material had not yet reached its plateau value.

The viscosity results (Fig. 3) are not in full agreement with the results of previous studies (Winuprasith and Suphantharika 2013), which showed that viscosity decreased with the number of homogenization passes. While this was found for the TEMPO-treated samples, the enzymatically-treated samples exhibited a reversed trend because these samples had not yet reached their maximum value, after which the viscosity deteriorated. Moreover, Zhang *et al.* (2012) showed that the viscosity increases with charge density, validating the higher values observed in the TEMPO-treated samples. The highest viscosity of TEMPO one pass is explained by larger aggregates acting as network nodes (Shogren *et al.* 2011). It was not possible to obtain stable values for nanopulp due to the inhomogeneity of the sample.

DLS measurements revealed that the hydrodynamic radii of the particles found in the supernatants varied depending on the number of passes and the pretreatment (Table 1). Higher hydrodynamic radii correspond to a greater amount of fibrillar aggregates. However, this should not be confused with the actual length of the cellulose nanofibers, because the hydrodynamic radius is affected by the surface charge density and ionic strength of the liquid. TEMPO one pass had an 8 wt. % decrease in yield when the rotational force was increased from 9800 to 20000 rcf, which coincides with the results from DLS and confirms that TEMPO one pass contained a significant amount of fibrillar aggregates. This further shows that supernatants after centrifugation at 9800 rcf can withhold nanoparticles of varying size. AFM image analysis, as shown in Fig. 4, of the supernatants confirmed that the supernatant of the different samples contained a variety of size fractions.

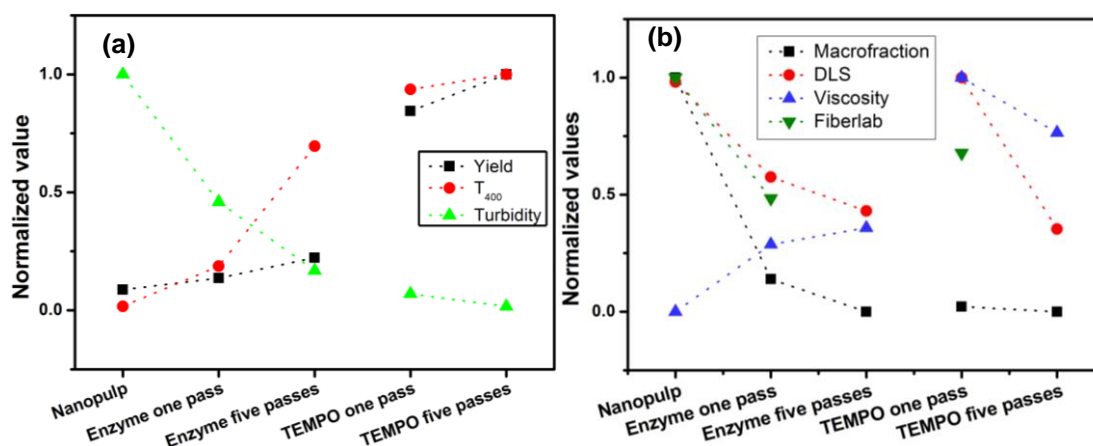


**Fig. 3.** Correlation graph of normalized values for (a) yield, turbidity, and transmittance (at  $T_{400}$ ) and (b) macro-fraction, hydrodynamic radius (DLS), viscosity, and size average (FiberLab). The samples are ordered from the least disintegrated (nanopulp) to the highest degree of disintegration (TEMPO five passes) on the horizontal axis.

The incline between points of the same pretreatment in Fig. 3(a) corresponds to the sensitivity within this region for the specific method, with a steeper incline representing greater sensitivity. This means that the macro-fraction is best used within the region of less disintegrated qualities (in this case, nanopulp and enzyme one pass) and is inadequate for more disintegrated qualities. Turbidity exhibited the highest sensitivity for less disintegrated qualities, and transmittance ( $T_{400}$ ) had the highest sensitivity within the

region of enzymatically-treated samples. Centrifugation had the lowest overall sensitivity, although it had the same sensitivity following both types of pretreatments. Fig. 3(b) shows that the viscosity may be used in certain intervals of samples with the same pretreatment. However, viscosity cannot be used to compare samples with different pretreatments. FiberLab was only applicable for poor disintegration. In the case of TEMPO one pass, only half of the fibers could be measured in the other samples. The hydrodynamic radius is largely affected by the charge density, which is visible in the graph.

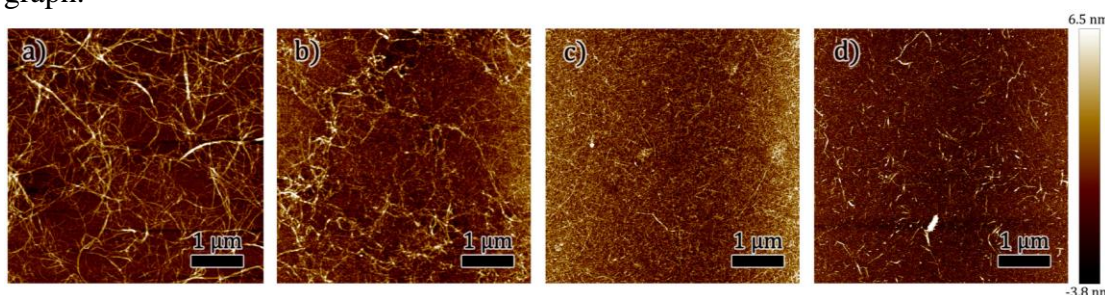


**Fig. 4.** AFM images of supernatants after 24 h adsorption: a) Enzyme one and five pass showed no discernable difference between the samples, with mainly fibrils and microfibrils visible; b) TEMPO one pass had a coarse network of nanofibers; c) TEMPO five passes presented a fine network of cellulose nanofibers; and d) nanopulp contained nanofibers and shattered fragments similar to CNC.

**Table 1.** Summary of Results from the Various Methods

Method	Nanopulp	Enzyme one pass	Enzyme five passes	TEMPO one pass	TEMPO five passes
Yield (wt. %)	8.7	13.6±0.1	22.2±0.1	84.2±0.2	99.7±0.1
Hydrodynamic radius RH (nm)	862.7±19.5	506.4±52	378.3±23	879.3±175	310.6±43.5
Macro fraction (wt. %)	59.8	8.3	0	1.3	0
FiberLab, Length-weighted length (μm)	310	150	-	210	-
Transmittance ( $T_{400}$ )	1.7	18.5	68.7	92.4	98.7
Turbidity (NTU)	284±11.5	130.5±6	47.7±0.8	19.8±0.5	4.6±0.9
Viscosity (mPas)	4±4	1.59±0.05	1.98±0.05	5.53±0.6	4.23±0.2
Energy per yield of nanomaterial (MWh/ton)	7.8	50	110	8	25

Average length values were determined in FiberLab. Due to the rapid sedimentation of nanopulp, no stable values could be obtained during turbidity and transmittance measurements, so instead, the values shown are from homogenized, dispersed nanopulp. The deviation from the average is shown for the samples with at least 3 measured points.

For rapid measurement, only turbidity or transmittance is viable, as shown in Table 2. These measurements could also be adapted for on-line measurement. Although both methods should preferably be used on less disintegrated samples, they can be applied to more disintegrated samples effectively. Centrifugation should be used to estimate the yield of nanofibers. However, care must be taken when analyzing the results because the supernatant fraction is inhomogeneous. The macro-fraction can only be used for poorly disintegrated qualities, and applying FiberLab on these qualities may give indications as to the macroscopic changes in the sample. DLS should only be used in addition to other methods when comparing different samples. AFM should only be applied when further studies of the quality are required.

**Table 2.** Summary of the Different Methods Considering Their Equipment Cost, Size, Time Requirements, and Range of Efficiency

Method	Approximate equipment cost	Equipment size	Required time	Most efficient
Centrifugation	\$300 to 1.4k <sup>1</sup>	Small to large	1 to 2 days	All
Turbidity	\$4 to 9k <sup>2</sup>	Small	<1 h	Low disintegration
Spectrophotometer (transmittance)	\$12k <sup>1</sup>	Medium	<1 h	Low disintegration
BDDRJ (Macro-fraction)	\$900 <sup>3</sup>	Small	1 to 2 days	Only low disintegration
Zetasizer (DLS)	\$50k <sup>4</sup>	Medium	2 h	Centrifugal supernatants
Atomic force microscopy	\$130k <sup>5</sup>	Medium	several days	All

<sup>1</sup> VWR International <sup>2</sup> HACH <sup>3</sup> Paper Research Materials Inc. <sup>4</sup> Malvern <sup>5</sup> Bruker

Equipment size: Small represents portable-to-tabletop sizes, medium is a tabletop connected with a computer, and large is an entire dedicated room. Required time includes the preparation of the samples and analysis of the results.

## CONCLUSIONS

1. Centrifugation provides quantitative values of a sample's nanomaterial content and works well as a standalone measurement and qualitative measurements were performed using a tabletop centrifuge, further promoting the method as a simple, standalone measurement method for quality or degree of fibrillation.
2. DLS measurements and AFM have shown that the supernatant fraction is inhomogeneous and also that the supernatant fraction contains different substituents in the differently-treated samples.
3. Turbidity is straightforward and capable of measuring significantly smaller differences in fibrillation for less fibrillated qualities than centrifugation. It initially increases with disintegration degree until a limit is reached at which it starts to decline, indicating that undetectable particles are being created. Undetectable particles are also created in the early stages of disintegration in materials such as the nanopulp. This leads to a small decrease in turbidity, even if the quality has yet to

reach its maximum. This effect suppresses the maximum turbidity, making it difficult to determine.

4. Turbidity should preferably be correlated to other measuring techniques, such as centrifugation.
5. Transmittance has similar strengths and weaknesses as the turbidity, and measurements from both methods were correlated with yield. The area of highest sensitivity is within the region of less disintegration.
6. Continued mechanical disintegration increased the amount of energy per nanomaterial yielded in both enzymatically- and TEMPO-treated samples.

## ACKNOWLEDGMENTS

This work was made possible by Valmet Corporation and supported by FORIC. Professors Tom Lindström and Lars Wågberg are acknowledged for their valuable advice, and Olof Melander, of Valmet, is thanked for his involvement in the project.

## REFERENCES CITED

- Abe, K., Iwamoto, S., and Yano, H. (2007). "Obtaining cellulose nanofibers with a uniform width of 15 nm from wood," *Biomacromolecules* 8(10), 3276-3278. DOI: 10.1021/bm700624p
- Alemdar, A., and Sain, M. (2008). "Isolation and characterization of nanofibers from agricultural residue - Wheat straw and soy hulls," *Bioresour. Technol.* 99(6), 1664-1671. DOI: 10.1016/j.biortech.2007.04.029
- Ankerfors, M. (2012). "Microfibrillated cellulose: Energy-efficient preparation techniques and key properties," Royal Institute of Technology, Innventia.
- Aulin, C., Gällstedt, M., and Lindström, T. (2010). "Oxygen and oil barrier properties of microfibrillated cellulose films and coatings," *Cellulose* 17(3), 559-574. DOI: 10.1007/s10570-009-9393-y
- Beck-Candanedo, S., Roman, M., and Gray, D. G. (2005). "Effect of reaction conditions on the properties and behavior of wood cellulose nanocrystal suspensions," *Biomacromolecules* 6(2), 1048-1054. DOI: 10.1021/bm049300p
- Blackwell, J., and Kolpak, F. J. (1975). "The cellulose microfibril as an imperfect array of elementary fibrils," *Macromolecules* 8(3), 322-326. DOI: 10.1021/ma60045a015
- Brinchi, L., Cotana, F., Fortunati, E., and Kenny, J. M. (2013). "Production of nanocrystalline cellulose from lignocellulosic biomass: Technology and applications," *Carbohydrate Polymers* 94(1), 154-169. DOI: 10.1016/j.carbpol.2013.01.033
- Chakraborty, A., Sain, M., and Kortschot, M. (2005). "Cellulose microfibrils: A novel method of preparation using high shear refining and cryocrushing," *Holzforschung* 59(1), 102-107. DOI: 10.1515/HF.2005.016
- Chatterjee, P. K., and Makoui, K. B. (1987). "Freeze dried microfibrillar cellulose," European Patent EP 0125850 B1

- Chinga-Carrasco, G. (2013). "Optical methods for the quantification of the fibrillation degree of bleached MFC materials," *Micron* 48, 42-48. DOI: 10.1016/j.micron.2013.02.005
- Chinga-Carrasco, G., Averianova, N., Gibadullin, M., Petrov, V., Leirset, I., and Syverud, K. (2013). "Micro-structural characterisation of homogeneous and layered MFC nano-composites," *Micron* 44, 331-338. DOI: 10.1016/j.micron.2012.08.005
- Dong, X. M., Kimura, T., Revol, J. F., and Gray, D. G. (1996). "Effects of ionic strength on the isotropic-chiral nematic phase transition of suspensions of cellulose crystallites," *Langmuir* 12(8), 2076-2082. DOI: 10.1021/la950133b
- Elazzouzi-Hafraoui, S., Nishiyama, Y., Putaux, J. L., Heux, L., Dubreuil, F., and Rochas, C. (2008). "The shape and size distribution of crystalline nanoparticles prepared by acid hydrolysis of native cellulose," *Biomacromolecules* 9(1), 57-65. DOI: 10.1021/bm700769p
- Eriksen, O., Syverud, K., and Gregersen, O. (2008). "The use of microfibrillated cellulose produced from kraft pulp as strength enhancer in TMP paper," *Nord. Pulp Paper Res.* 23(3), 299-304.
- Evans, R., and Wallis, A. F. A. (1989). "Cellulose molecular-weights determined by viscometry," *Journal of Applied Polymer Science* 37(8), 2331-2340. DOI: 10.1002/app.1989.070370822
- Fall, A., Lindström, S., Sprakel, J., and Wågberg, L. (2013). "A physical cross-linking process of cellulose nanofibril gels with shear-controlled fibril orientation," *Soft Matter* 9(6), 1852-1863. DOI: 10.1039/c2sm27223g
- Fall, A., Lindström, S., Sundman, O., Ödberg, L., and Wågberg, L. (2011). "Colloidal stability of aqueous nanofibrillated cellulose dispersions," *Langmuir* 27(18), 11332-11338. DOI: 10.1021/la201947x
- Frey-Wyssling, A., Mühlethaler, K., and Wyckoff, R. W. G. (1948). "Mikrofibrillenbau der pflanzlichen Zellwände," *Experientia* 4(12), 475-476. DOI: 10.1007/BF02164504
- Fukuzumi, H., Saito, T., Iwata, T., Kumamoto, Y., and Isogai, A. (2009). "Transparent and high gas barrier films of cellulose nanofibers prepared by TEMPO-mediated oxidation," *Biomacromolecules* 10(1), 162-165. DOI: 10.1021/bm801065u
- Gousse, C., Chanzy, H., Cerrada, M. L., and Fleury, E. (2004). "Surface silylation of cellulose microfibrils: preparation and rheological properties," *Polymer* 45(5), 1569-1575. DOI: 10.1016/j.polymer.2003.12.028
- Hamad, W. Y., and Hu, T. Q. (2010). "Structure-process-yield interrelations in nanocrystalline cellulose extraction," *The Canadian Journal of Chemical Engineering* 88(3), 392-402. DOI: 10.1002/cjce.20298
- Helander, M., Zhu, H., Moser, C., Ståhlkranz, A., Söderberg, D., and Henriksson, G. L., M. (2012). "A novel nano cellulose preparation method and size fraction by cross flow ultra-filtration," *Current Organic Chemistry* 16(16), 1871-1875.
- Henriksson, G., Lawoko, M., Christiernin, M., and Henriksson, M. (2005). "Monocomponent endoglucanases an excellent tool in wood chemistry and pulp processing," 59<sup>th</sup> Appita Annual Conference and Exhibition: Incorporating the 13th ISWFPC
- Henriksson, G., Henriksson, M., Berglund, L. A., and Lindström, T. (2007a). "An environmentally friendly method for enzyme assisted preparation of microfibrillated cellulose (MFC) nanofibers," *European Polymer Journal* 43(8), 3434-3441. DOI: 10.1016/j.eurpolymj.2007.05.038

- Henriksson, M., Henriksson, G., Berglund, L. A., and Lindström, T. (2007b). "An environmentally friendly method for enzyme-assisted preparation of microfibrillated cellulose (MFC) nanofibers," *European Polymer Journal* 43(8), 3434-3441. DOI: 10.1016/j.eurpolymj.2007.05.038
- Herrick, F. W. (1984). "Process for preparation microfibrillated cellulose," US 4481077 A
- Herrick, F. W., Casebier, R. L., J. K. H., and Sandberg, K. R. (1983). "Microfibrillated cellulose: morphology and accessibility," *Journal of Applied Polymer Science: Applied Polymer Symposium* 37, 797-813.
- Heyn, A. N. (1969). "The elementary fibril and supermolecular structure of cellulose in soft wood fiber," *Journal of Ultrastructure Research* 26(1), 52-68.
- Hua, X., Laled, M., and Owston, T. (2011). "Cellulose nanofilaments and Method to Produce same," US Patent US 20110277947 A1.
- Isogai, A., Saito, T., and Fukuzumi, H. (2011). "TEMPO-oxidized cellulose nanofibers," *Nanoscale* 3(1), 71-85. 10.1039/C0NR00583E
- Iwamoto, S., Abe, K., and Yano, H. (2008). "The effect of hemicelluloses on wood pulp nanofibrillation and nanofiber network characteristics," *Biomacromolecules* 9(3), 1022-1026. DOI: 10.1021/bm701157n
- Iwamoto, S., Nakagaito, A. N., and Yano, H. (2007). "Nano-fibrillation of pulp fibers for the processing of transparent nanocomposites," *Applied Physics A: Materials Science & Processing* 89(2), 461-466. DOI: 10.1007/s00339-007-4175-6
- Jin, H., Nishiyama, Y., Wada, M., and Kuga, S. (2004). "Nanofibrillar cellulose aerogels," *Colloids and Surfaces A: Physicochemical and Engineering Aspects* 240(1-3), 63-67. DOI: 10.1016/j.colsurfa.2004.03.007
- Jukka, A., Peiponen, K. E., and Asakura, T. (2004). *UV-Visible Reflection Spectroscopy of Liquids*, Springer Series in Optical Sciences, Vol. 92.
- Katz, S., Scallan, A. M., and Beatson, R. P. (1984). "The determination of strong and weak acidic groups in sulfite pulps," *Svensk Papperstidning* 87(6), 48-53.
- Kaushika, A., and Singh, M. (2011). "Isolation and characterization of cellulose nanofibrils from wheat straw using steam explosion coupled with high shear homogenization," *Carbohydrate Research* 346(1), 76-85. DOI: 10.1016/j.carres.2010.10.020
- Klemm, D., Heublein, B., Fink, H. P., and Bohn, A. (2005). "Cellulose: Fascinating biopolymer and sustainable raw material," *ChemInform* 44(22), 3358-3393. DOI: 10.1002/chin.200536238
- Klemm, D., Kramer, F., Moritz, S., Lindström, T., Ankerfors, M., Gray, D., and Dorris, A. (2011). "Nanocelluloses: A new family of nature-based materials," *Angewandte Chemie, International Edition* 50(24), 5438-5466. DOI: 10.1002/anie.201001273
- Langlois, B., Benchimol, J., Guerin, G., Vincent, I., Senechal, A., and Cantiani, R. (2002). "Fluid comprising cellulose nanofibrils and its use for oil mining," US Patent US 6348436 B1
- Lapierre, L., Bouchard, J., and Berry, R. (2006). "On the relationship between fibre length, cellulose chain length and pulp viscosity of a softwood sulfite pulp," *Holzforschung* 60(4), 372-377. DOI: 10.1515/HF.2006.058
- Meier, H. (1962). "Chemical and morphological aspects of the fine structure of wood," *Pure and Applied Chemistry* 5, 37-52.

- Meshitsuka, G., and Isogai, A. (1995). "Chemical structures of cellulose, hemicelluloses, and lignin," *Chemical Modification of Lignocellulosic Materials*. CRC Press, New York, 11-34.
- Mishra, S. P., Thirree, J., Manent, A.-S., Chabot, B., and Daneault, C. (2011). "Ultrasound-catalyzed TEMPO-mediated oxidation of native cellulose for the production of nanocellulose: Effect of process variables," *BioResources* 6(1), 121-143.
- Moberg, T., and Rigdahl, M. (2012). "On the viscoelastic properties of microfibrillated cellulose (MFC) suspensions," *Annual Transactions of the Nordic Rheology Society*, 123-130.
- Mühlenthaler, K. (1949). "Electron micrographs of plant fibers," *Biochimica et Biophysica Acta* 3(15), 15-25.
- Nickerson, R.F. and Harble, J. A. (1947). "Cellulose intercrystalline structure," *Industrial & Engineering Chemistry Research* 39(11), 1507-1512.
- Ohad, I., and Danon, D. (1964). "On the dimensions of cellulose microfibrils," *The Journal of Cell Biology* 22(1), 302-305.
- Pääkkö, M., Ankerfors, M., Kosonen, H., Nykänen, A., Ahola, S., Osterberg, M., Ruokolainen, J., Laine, J., Larsson, P. T., Ikkala, O., and Lindström, T. (2007). "Enzymatic hydrolysis combined with mechanical shearing and high-pressure homogenization for nanoscale cellulose fibrils and strong gels," *Biomacromolecules* 8(6), 1934-1941. DOI: 10.1021/bm061215p
- Peterlin, A., and Ingram, P. (1970). "Morphology of secondary wall fibrils in cotton," *Textile Research Journal* 40(4), 345-354.
- Pokhrel, D., and Viraraghavan, T. (2004). "Treatment of pulp and paper mill wastewater—A review," *Science of the Total Environment* 333(1-3), 37-58. DOI: 10.1016/j.scitotenv.2004.05.017
- Qua, E. H., Hornsby, P. R., Sharma, H. S. S., and Lyons, G. (2011). "Preparation and characterisation of cellulose nanofibres," *Journal of Material Science* 46(18), 6029-6045. DOI: 10.1007/s10853-011-5565-x
- Rezayati Charani, P., Dehghani-Firouzabadi, M., Afra, E., and Shakeri, A. (2013). "Rheological characterization of high concentrated MFC gel from kenaf unbleached pulp," *Cellulose* 20(2), 727-740. DOI: 10.1007/s10570-013-9862-1
- Rånby, B. G. (1949). "Aqueous colloidal solutions of cellulose micelles," *ACTA Chemica Scandinavica* 3(3), 649-650.
- Rånby, B. G. (1951). "The colloidal properties of cellulose micelles," *Discussions of the Faraday Society* 11, 158-164.
- Saito, T., Hirota, M., Tamura, N., Kimura, S., Fukuzumi, H., Heux, L., and Isogai, A. (2009). "Individualization of nano-sized plant cellulose fibrils by direct surface carboxylation using TEMPO catalyst under neutral conditions," *Biomacromolecules* 10(7), 1992-1996. DOI: 10.1021/bm900414t
- Saito, T., Kimura, S., Nishiyama, Y., and Isogai, A. (2007). "Cellulose nanofibers prepared by TEMPO-mediated oxidation of native cellulose," *Biomacromolecules*, 8(8), 2485-2491. DOI: 10.1021/bm0703970
- Saito, T., Nishiyama, Y., Putaux, J., Vignon, M., and Isogai, A. (2006). "Homogeneous suspensions of individualized microfibrils from TEMPO-catalyzed oxidation of native cellulose," *Biomacromolecules* 7(6), 1687-1691. DOI: 10.1021/bm060154s

- Shogren, R. L., Peterson, S. C., Evans, K. O., and Kenar, J. A. (2011). "Preparation and characterization of cellulose gels from corn cobs," *Carbohydrate Polymers* 86(3), 1351-1357. DOI: 10.1016/j.carbpol.2011.06.035
- Siró, I., and Plackett, D. (2010). "Microfibrillated cellulose and new nanocomposite materials: A review," *Cellulose* 17(3), 459-494. DOI: 10.1007/s10570-010-9405-y
- Spence, K. L., Venditti, R. A., Habibi, Y., Rojas, O. J., Pawlak, J. J. (2010). "The effect of chemical composition on microfibrillar cellulose films from wood pulps: Mechanical processing and physical properties," *Bioresour. Technol.* 101(15), 5961-5968. DOI: 10.1016/j.biortech.2010.02.104
- Tanaka, A., Hjelt, T., Sneek, A., and Korpela, A. (2012a). "Fractionation of nanocellulose by foam filter," *Separation Science and Technology* 47(12), 1771-1776. DOI: 10.1080/01496395.2012.661825
- Tanaka, A., Seppanen, V., Houni, J., and Sneek, A. A. P., P. (2012b). "Nanocellulose characterization with mechanical fractionation," *Nordic Pulp and Paper Research Journal* 27(4), 689-694.
- Tejado, A., Alam, M. N., Antal, M., Yang, H., and van de Ven, T. G. M. (2012). "Energy requirements for the disintegration of cellulose fibers into cellulose nanofibers." *Cellulose* 19(3), 831-842. DOI: 10.1007/s10570-012-9694-4
- Turbak, A. F., Snyder, F. W., and Sandberg, K. R. (1983). "Microfibrillated cellulose, a new cellulose product: Properties, uses, and commercial potential," *Journal of Applied Polymer Science: Applied Polymer Symposium* 37, 815-827.
- Wang, B., and Sain, M. (2007). "Isolation of nanofibers from soybean sources and their reinforcing capability on synthetic polymers," *Composites Science and Technology* 67(11-12), 2521-2527. DOI: 10.1016/j.compscitech.2006.12.015
- Wilson, S. M., Burton, R. A., Collins, H. M., Doblin, M. S., Pettolino, F. A., Shirley, N., Fincher, G. B., and Bacic, A. (2012). "Pattern of deposition of cell wall polysaccharides and transcript abundance of related cell wall synthesis genes during differentiation in barley endosperm," *Plant Physiology* 159(2), 655-670. DOI: 10.1104/pp.111.192682
- Winuprasith, T., and Supphantharika, M. (2013). "Microfibrillated cellulose from mangosteen (*Garcinia mangostana* L.) rind: Preparation, characterization, and evaluation as an emulsion stabilizer," *Food Hydrocolloids* 32(2). DOI: 10.1016/j.foodhyd.2013.01.023
- Wågberg, L., Decher, G., Norgren, M., Lindström, T., Ankerfors, M., and Axnäs, K. (2008). "The build-up of polyelectrolyte multilayers of microfibrillated cellulose and cationic polyelectrolytes," *Langmuir* 24(3), 784-795.
- Zhang, J., Song, H., Lin, L., Zhuang, J., Pang, C., and Liu, S. (2012). "Microfibrillated cellulose from bamboo pulp and its properties," *Biomass and Bioenergy* 39(SI), 78-83. DOI: 10.1016/j.biombioe.2010.06.013
- Zimmermann, T., Pöhler, E., and Geiger, T. (2004). "Cellulose fibrils for polymer reinforcement," *Advanced Engineering Materials* 6(9), 754-761. DOI: 10.1002/adem.200400097

Article submitted: January 9, 2015; Peer review completed: February 16, 2015; Revised version received and accepted: February 18, 2015; Published: February 25, 2015.  
DOI: 10.15376/biores.10.2.2360-2375